Supporting Information

Stimuli-responsive micro/nanoporous hairy skin for adaptive thermal insulation and infrared camouflage

*Ayoung Choe, Jeonghee Yeom, Yeju Kwon, Youngoh Lee, Young-Eun Shin, Jinyoung Kim, and Hyunhyub Ko**

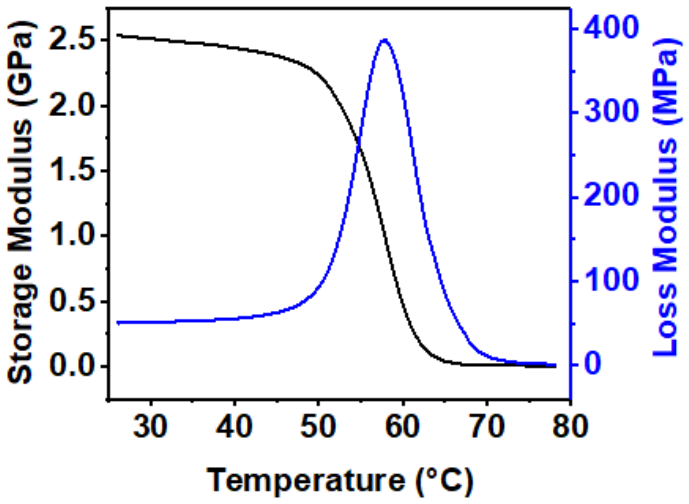

Figure S1. Storage and loss moduli of the nonporous PLA film with increasing temperature. The sample dimension was 18.5 × 6.12 × 0.23 mm^3 and the measurement was done from 26 to 78 °C at a heating rate of 2 °C min^{-1} and a frequency of 1 Hz.

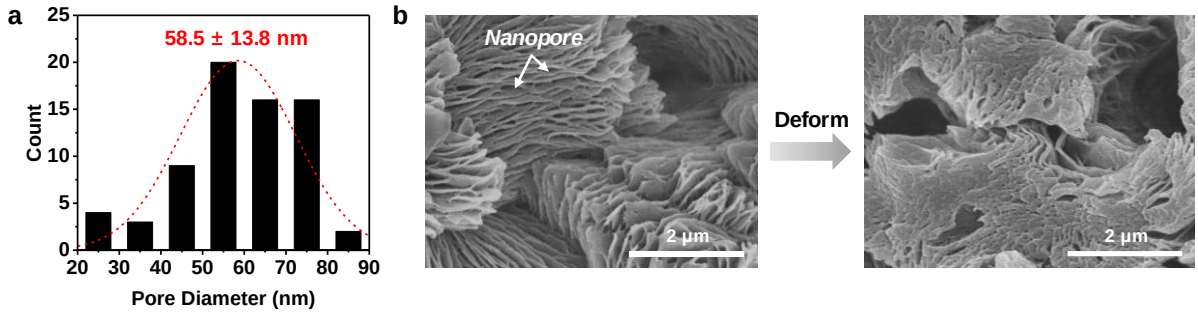

Figure S2. Changes in nanopore sizes of the porous SMP. a) Histogram of the nanopore sizes in the porous SMP. The mean pore diameter is 58.5 nm. b) Cross-sectional SEM images of the original (left) and the deformed (right) nanopores in the hierarchical micro/nanoporous SMP.

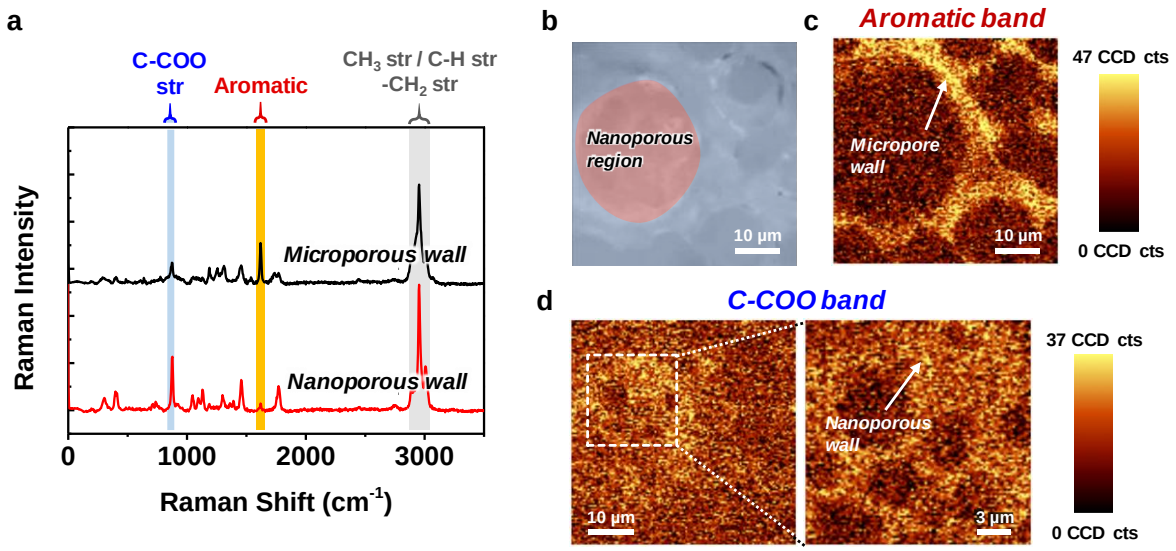

Figure S3. Composition of the hierarchical micro/nanoporous SMP. (a) Raman spectra of the porous SMP on microporous and nanoporous walls, respectively. 'str' means the stretching mode in Raman spectra. (b) Optical microscopy image of the porous SMP. The arrow indicates the nanoporous region in the hierarchical micro/nanoporous structure. Raman mapping images of the (c) aromatic and (d) C-COO bands (left) for the same region of (b). The Raman mapping image of the C-COO band in the higher resolution (d, right).

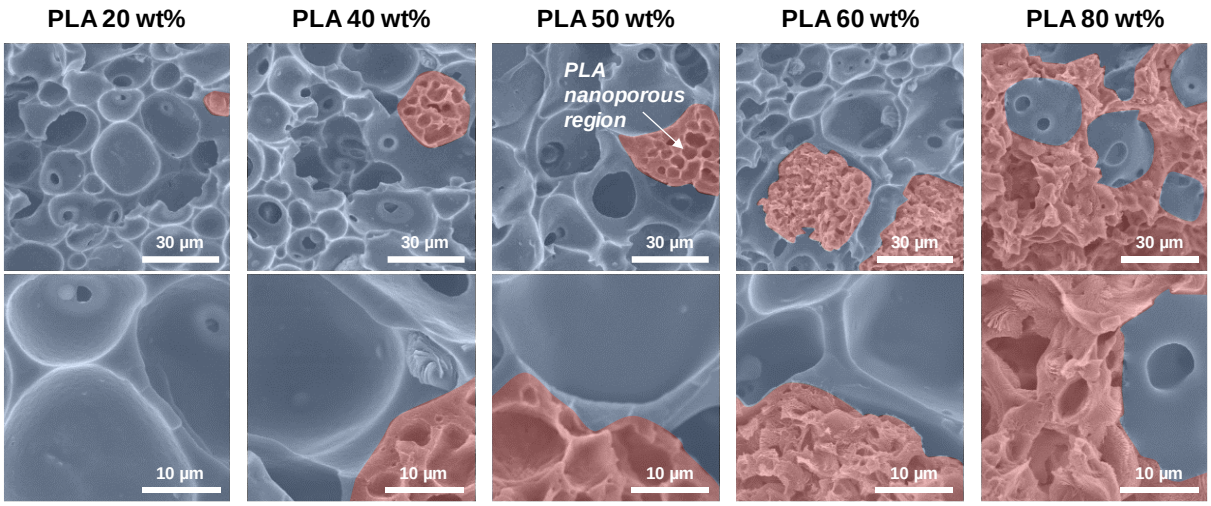

Figure S4. Cross-sectional SEM images of porous SMPs with different PLA concentrations from 20 to 80 wt%. The arrow indicates the PLA-dominant nanoporous region.

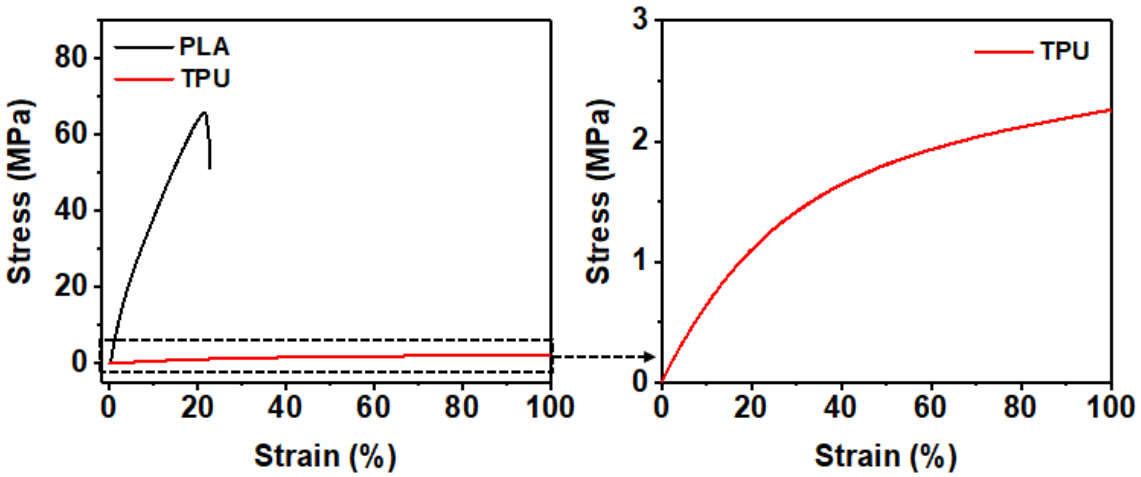

Figure S5. Tensile stress-strain curves of nonporous PLA and TPU films. The right-hand side graph is the magnified view of the stress-strain curve of TPU. The stretching tests were performed at a speed of 0.1 mm s^{-1}.

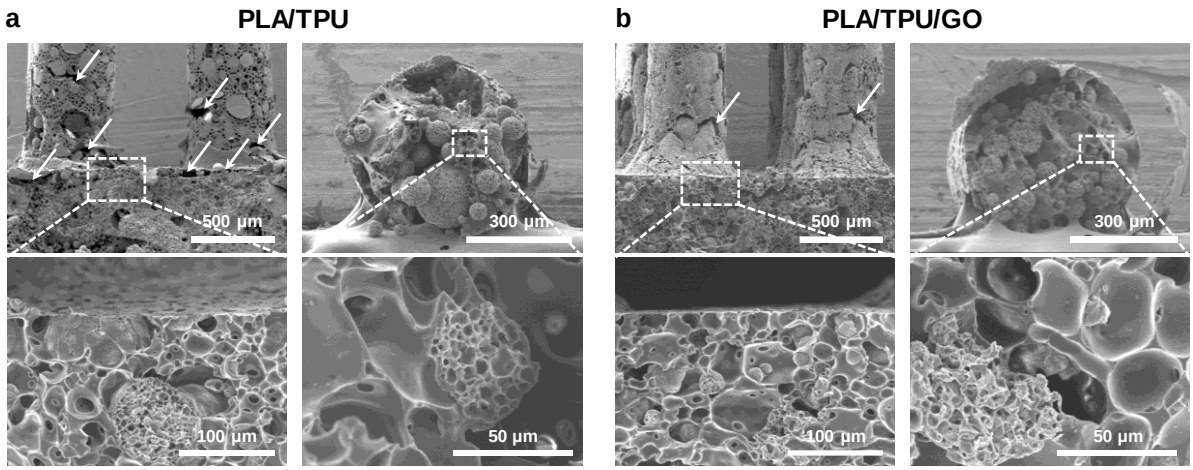

Figure S6. Changes in structures of the hairy SMPs after adding GOs. Cross-sectional SEM images of the hairy (a) PLA/TPU and (b) PLA/TPU/GO samples for the film (left column) and the pillar (right column) position, respectively. White arrows indicate cracks.

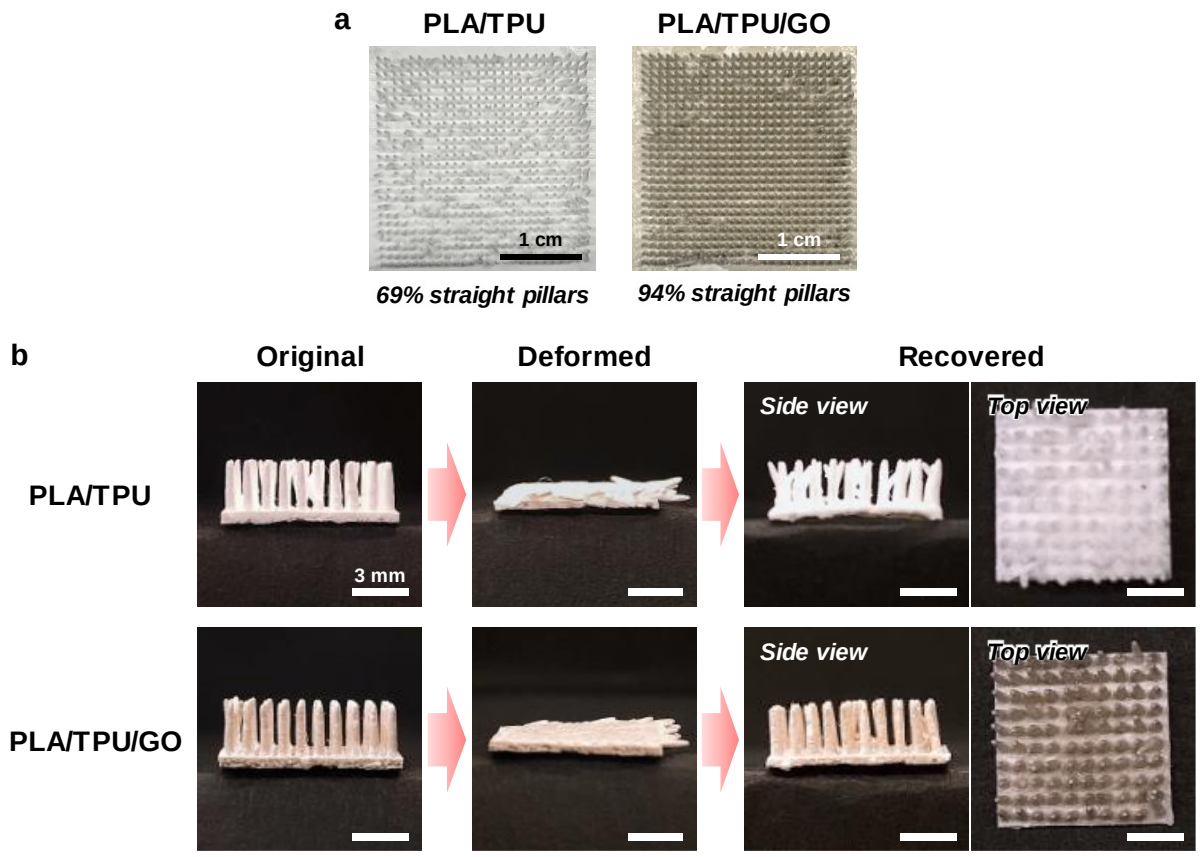

Figure S7. Shape memory properties of the hairy SMPs. (a) Top view photographs of the hairy PLA/TPU (left) and PLA/TPU/GO (right) samples. The hairy PLA/TPU and PLA/TPU/GO samples have 69% and 94% straight pillars, respectively. (b) Photographs of the hairy PLA/TPU (upper row) and PLA/TPU/GO (lower row) samples in the original, deformed, and recovered states, respectively. Scale bars in (b) are 3 mm.

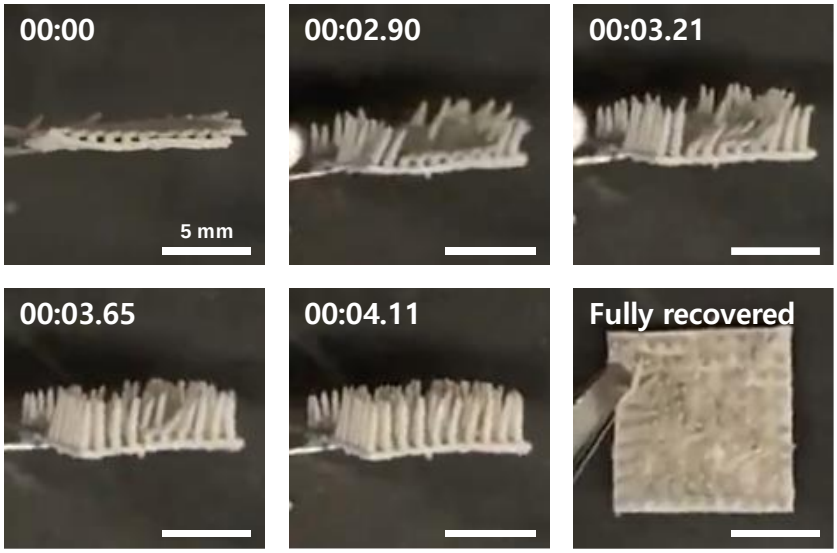

Figure S8. Photographs of the hairy PLA/TPU/GO sample with 1 × 1 cm^2 size during the shape recovery process in the 70 °C water bath. The images show the side view of sample to clearly show the shape of pillars except the last one which show the top view of the sample after finishing the recovery process. The numbers on the top left of each photograph indicate the time that elapsed since the recovery starts. Scale bars are 5 mm.

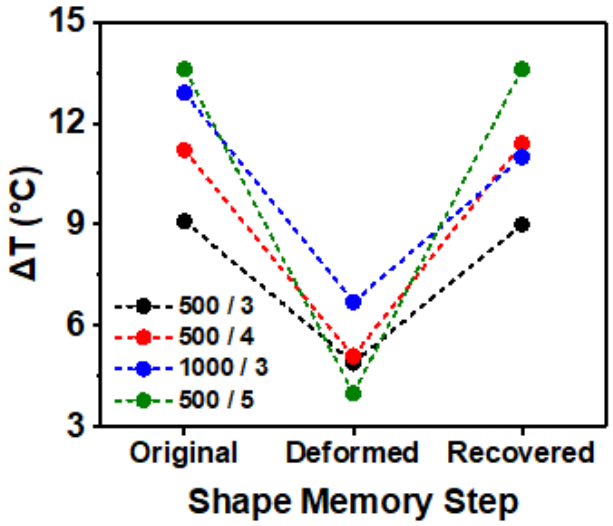

Figure S9. Change of ΔT for hairy SMPs with different pillar diameters (μm) and aspect ratios (diameter / aspect ratio) during the shape memory test. The ΔT values of the hairy SMP were measured on a hot plate at 60 °C.

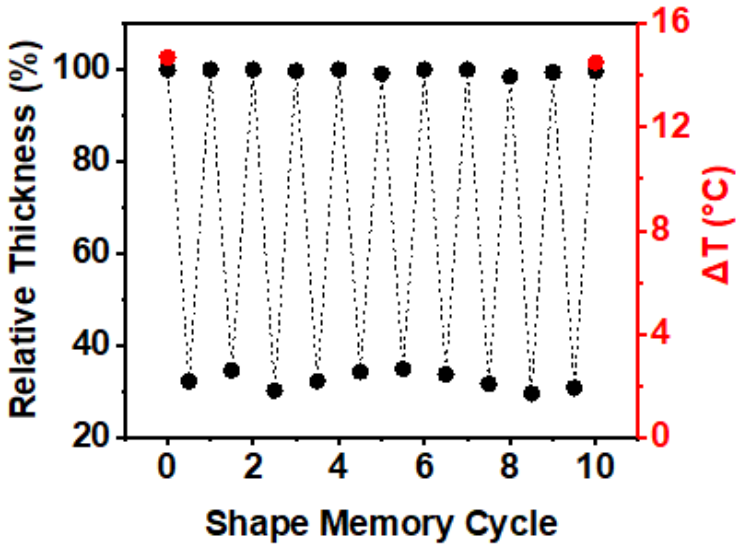

Figure S10. Change in the relative thickness and ΔT values of the hairy SMP during repetitive shape memory tests. The ΔT values of the hairy SMP were measured before the shape memory test and after the 10th cyclic test on a hot plate at 60 °C.

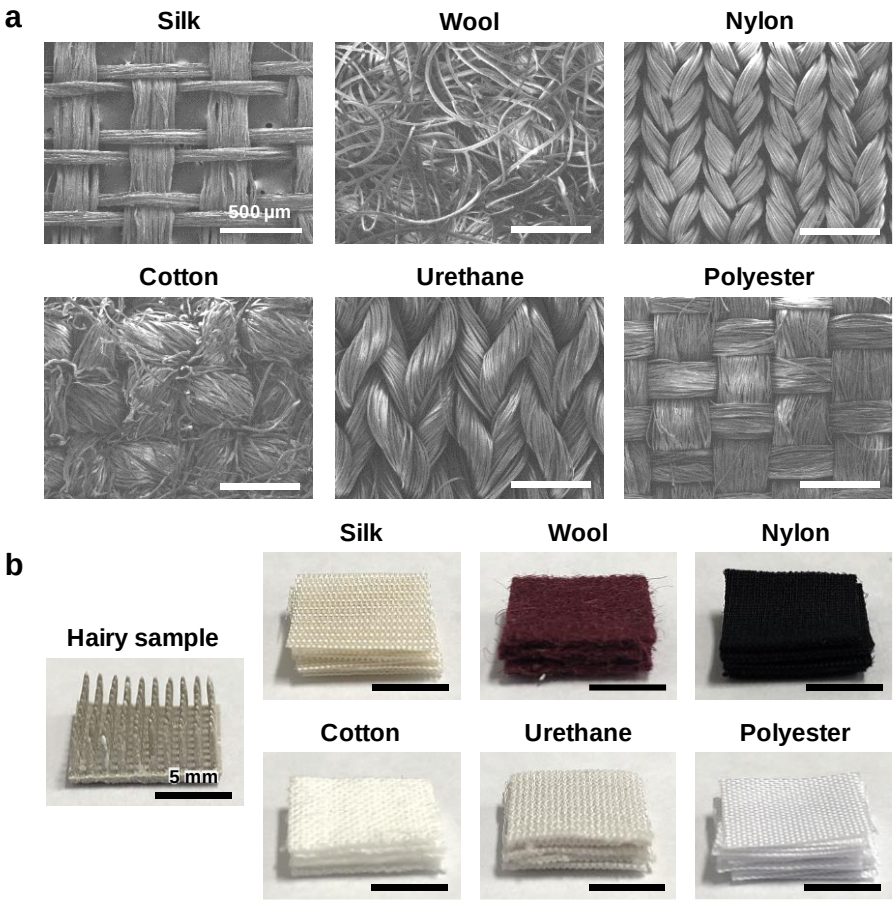

Figure S11. Comparison of the thermal insulation of the hairy SMP to those of commercial textiles. (a) SEM images of commercial textiles. Scale bars in (a) are 500 µm. (b) Photographs of the hairy sample and commercial textiles with thickness of 3 mm. Scale bars in (b) are 5 mm.

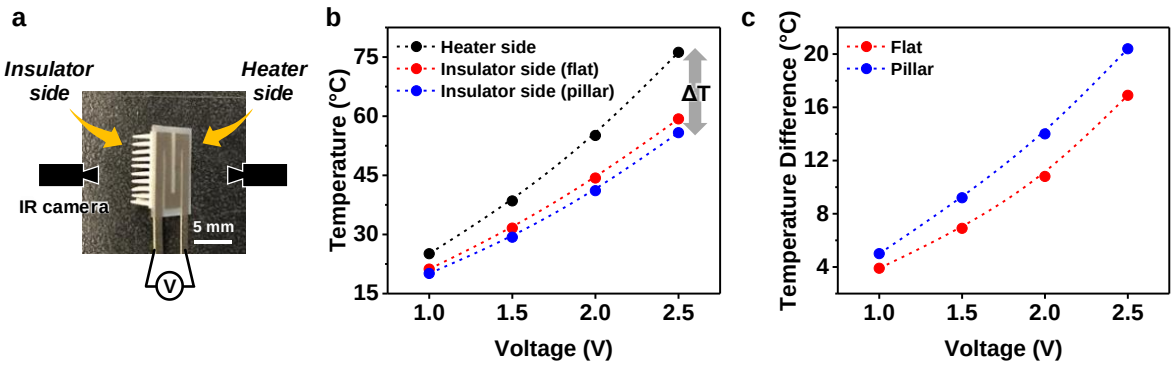

Figure S12. Integration of the hairy SMP and the Joule heater. (a) Photograph of the hairy SMP attached to the Joule heater made of nickel/copper film. (b) Plot of temperature versus voltage for heater and insulator (flat and pillar samples) sides. (c) Plot of temperature difference between heater and insulator sides for flat and pillar samples.

Table S1. Previous studies of thermal insulation.

Material	Pore size	Thermal insulation (Temperature difference)	Tunability of thermal insulation	Shape fixability	Ref.
Fluoroalklsilane/PDMS/ AgNWs/Nylon cloth	<300 nm	ΔT = 4.6 °C (37 °C plate) ΔT = ~10 °C (50 °C plate)	x	x	1
3D graphene foam	~35 μm	N/A	O	x	2
Silicone carbide foam	5~50 μm	N/A	x	x	3
PS/SiO_2 NPs/AgNWs/Glass	15 nm	ΔT = ~10 °C (60 °C plate)	x	x	4
Polyacrylonitrile/CNT/ Fe_3O_4 aerogel	70~130 μm & 4 nm	ΔT = 14.42 °C (50 °C plate)	x	x	5
Cellulose nanofibrillar network/mesoporous polymethylsilsesquioxane	~20 nm	ΔT = 8.8 °C (33 °C plate) ΔT = 28.7 °C (55.2 °C plate)	x	x	6
Porous silk fiber & textile	~30 μm	ΔT = 15 °C (60 °C plate)	x	x	7
Cellulose nanofibers/GO/ Sepiolite nanorods foam	~20 μm & 3 nm	N/A	x	x	8
CNT-coated triacetate-cellulose bimorph textile	A few hundreds of μm	N/A	x	x	9
Pillar-patterned porous PLA/TPU	Hierarchical micro/nanopores	ΔT = 18.6 °C (63.5 °C plate)	O	O	**This work**

References

1 Y. Guo, K. Li, C. Hou, Y. Li, Q. Zhang, H. Wang, *ACS Appl. Mater. Interfaces,* 2016, **8**, 4676-4683.

2 Q. Zhang, M. Hao, X. Xu, G. Xiong, H. Li, T. S. Fisher, *ACS Appl. Mater. Interfaces,* 2017, **9**, 14232-14241.

3 C. Liang, Z. Wang, L. Wu, X. Zhang, H. Wang, Z. Wang, *ACS Appl. Mater. Interfaces,* 2017, **9**, 29950-29957.

4 J.-G. Lee, S. An, T.-G. Kim, M.-W. Kim, H.-S. Jo, M. T. Swihart, A. L. Yarin, S. S. Yoon, *ACS Appl. Mater. Interfaces,* 2017, **9**, 35325-35332.

5 Y. Li, X. Liu, X. Nie, W. Yang, Y. Wang, R. Yu, J. Shui, *Adv. Funct. Mater.,* 2019, **29**, 1807624.

6 J. Zhang, Y. Cheng, M. Tebyetekerwa, S. Meng, M. Zhu, Y. Lu, *Adv. Funct. Mater.,* 2019, **29**, 1806407.

7 Y. Cui, H. Gong, Y. Wang, D. Li, H. Bai, *Adv. Mater.,* 2018, **30**, 1706807.

8 B. Wicklein, A. Kocjan, G. Salazar-Alvarez, F. Carosio, G. Camino, M. Antonietti, L. Bergström, *Nat. Nanotechnol.,* 2015, **10**, 277-283.

9 X. A. Zhang, S. Yu, B. Xu, M. Li, Z. Peng, Y. Wang, S. Deng, X. Wu, Z. Wu, M. Ouyang, Y. Wang, *Science,* 2019, **363**, 619-623.

Caption of Supplementary Video

Video S1 Dynamic thermal insulation of the hairy SMP. Real-time IR thermometer images of the hairy SMP attached on a polypropylene cup containing 40 °C water. The deformed hairy SMP was recovered by heating with a hair dryer. The speed of video is 4x.